

Quantum algorithm for the microcanonical Thermal Pure Quantum method

Kaito Mizukami¹ and Akihisa Koga¹

¹*Department of Physics, Tokyo Institute of Technology, Meguro, Tokyo 152-8551, Japan*

(Dated: August 20, 2023)

We present a quantum algorithm for the microcanonical thermal pure quantum (TPQ) method, which has an advantage in evaluating thermodynamic quantities at finite temperatures, by combining with some recently developed techniques derived from quantum singular value transformation. When the ground energy of quantum systems has already been obtained precisely, the multiple products of the Hamiltonian are efficiently realized and the TPQ states at low temperatures are systematically constructed in quantum computations.

I. INTRODUCTION

Quantum computer has been considered as a potential tool over the classical computations. One of the advantages in the quantum computations is the reduction of the computational cost to solve certain problems *e.g.* the prime factorizations [1] and linear algebraic calculations [2, 3]. Recently, many of such quantum algorithms have been unified together by a novel technique known as the quantum singular value transformation (QSVT) [4, 5], which allows one to perform a polynomial transformation of the singular values of a matrix embedded in a unitary matrix. This technique is expected to further accelerate the development of quantum algorithms. In the field of the condensed matter physics, the reduction of the computational memory representing the quantum state is also important to simulate the quantum many-body systems. When the $S = 1/2$ quantum spin model with the finite system size N is considered, each quantum state is represented by the vector with 2^N elements, which makes it hard to deal with the larger system on the classical computers. On the other hand, as for the quantum computer, each state is represented in terms of only N qubits. Since more than 100 qubits have been reported to be realized [6, 7], quantum computations are potential candidates for simulating the quantum systems in the thermodynamic limit.

One of the important applications is the simulation for the thermodynamic quantities at finite temperatures. It is known that, in the classical computations, the quantum Monte Carlo method is one of the powerful methods to treat the large system since thermodynamic quantities are evaluated by the random samplings in N spins. However, in the frustrated systems, serious minus sign problems appear at low temperatures, and thereby it is still hard to examine thermodynamic properties except for the special cases [8, 9]. Therefore, another tool is desired to discuss thermodynamic properties in the generic quantum spin systems with large clusters.

The Gibbs sampling algorithm on the quantum computer has been proposed [10], where the Gibbs state can be efficiently prepared. Another complementary method is the thermal pure quantum (TPQ) method [11, 12], where the thermal averages for the physical quantities are efficiently evaluated with a typical quantum state for the thermal equilibrium at finite temperature. Its quantum algorithm has recently been developed, where the TPQ states are represented by means of the imaginary time evolution [13–15]. These two algorithms are based on the canonical ensemble in the statistical mechan-

ics. On the other hand, the TPQ states for isolated systems, whose properties are described by the microcanonical ensemble, should be important [16], *e.g.* the effects of the disorders and real-time dynamics in finite systems. Therefore, as a complementary method, it is also instructive to construct the TPQ states in isolated systems by means of the quantum algorithm.

In the manuscript, we present a quantum algorithm for the microcanonical TPQ method [11]. In our scheme, a multiple product of the Hamiltonian for constructing the TPQ states is realized, by making advantages of some recently developed techniques derived from QSVT. We demonstrate that the squared norm of the TPQ state, deeply related to the complexity for the quantum simulations, decreases with increasing the number of iterations, but reaches a certain reasonable value if the precise value of the ground state energy is given as an input of parameters. This enables us to explore thermodynamic properties of quantum spin systems with the quantum computer.

The paper is organized as follows. In Sec. II, we briefly explain the TPQ method. In Sec. III, we explain quantum techniques used in our scheme. We introduce our TPQ scheme and clarify its complexity in Sec. IV. Some numerical results for the frustrated spin systems are also addressed. A summary is given in the last section.

II. THERMAL PURE QUANTUM METHOD

We consider an isolated quantum spin system with the lattice sites N , which is described by a Hamiltonian H , and assume that the dimension of the Hilbert space is $D = 2^N$. The TPQ state $|\psi\rangle$ is one of the typical states for a certain temperature, and the average in the equilibrium state for an operator A is simply evaluated as

$$\langle A \rangle = \frac{\langle \psi | A | \psi \rangle}{\langle \psi | \psi \rangle}. \quad (1)$$

This formula is exact in the thermodynamic limit as far as A is represented by low-degree polynomials of the local operators. It is known that, even in the small clusters, the TPQ method reasonably describes thermodynamic properties in the thermodynamic limit. An important point is that, in the TPQ method, one obtains the average without the diagonalization of the Hamiltonian H . Therefore, it has recently been applied to interesting systems such as the Heisenberg model on frustrated lattices [11, 12, 17–21] and the Kitaev models [22–29]

to discuss their thermodynamic properties.

Now, we briefly explain the microcanonical TPQ method [11]. Here, we denote the minimum and maximum eigenvalue of the Hamiltonian H by E_{\min} and E_{\max} , respectively. A TPQ state at $T \rightarrow \infty$ is simply given by a random state

$$|\psi_0\rangle = \sum_{i=1}^D c_i |i\rangle, \quad (2)$$

where $\{c_i\}$ is a set of random complex numbers satisfying $\sum_i |c_i|^2 = 1$ and $|i\rangle$ is an arbitrary orthonormal basis. By multiplying a certain TPQ state by the Hamiltonian, the TPQ states at lower temperatures are constructed. Then, the k th TPQ state is represented as [11]

$$|\psi_k\rangle = (L - H)|\psi_{k-1}\rangle = (L - H)^k |\psi_0\rangle, \quad (3)$$

where $L (> E_{\max})$ is a constant value. The internal energy \mathcal{E} and inverse temperature β are given as,

$$\mathcal{E}_k = \frac{\langle \psi_k | H | \psi_k \rangle}{\langle \psi_k | \psi_k \rangle}, \quad (4)$$

$$\beta_k = \frac{2k}{L - \mathcal{E}_k}. \quad (5)$$

Since the temperature has an intensive property, the number of the iterations k , which is proportional to the system size N , is needed to access a certain temperature. Thermodynamic quantities such as the specific heat and entropy are evaluated from the above quantities and the average of the operator A at the temperature $T_k (= 1/\beta_k)$ is obtained in eq. (1). Since the errors in the above formula decrease over the system size, a set of the TPQ states generated from a single initial state suffices for exploring thermodynamic properties in a sufficiently large system at finite temperatures.

A key of this method is that the TPQ states are iteratively constructed in terms of eq. (3). In the classical computation, the product between the Hamiltonian and TPQ state is easy to implement. By contrast, each state is described by the complex vector with D elements and thereby the feasible cluster size is restricted by the memory of the classical computer. On the other hand, one meets a distinct difficulty in quantum computations. Each TPQ state can be represented in terms of only N qubits, while multiple products in eq. (3) exponentially reduce the success probability in the TPQ method, which will be discussed later. This means that the simple TPQ simulation is hard to examine thermodynamic properties at low temperatures. In the following, combining with some techniques proposed recently, we present the efficient TPQ scheme to examine thermodynamic properties on the quantum computer.

III. MAIN TECHNIQUES

In this section, we explain several techniques based on the QSVT. In quantum computations, any operations should be described by the unitary operators. To operate the Hermite

Hamiltonian $H' (= L - H)$, we use the block-encoding technique. We here define a unitary matrix U , introducing the N_a -qubit ancillary register, as

$$\langle\langle 0|_a \otimes I_s \rangle\rangle U(|0\rangle_a \otimes I_s) = \frac{H'}{\alpha}, \quad (6)$$

where the index s (a) represents the system (ancillary) register, I is an identity matrix, and $\alpha > \|H'\| (= L - E_{\min})$ is a positive constant. Note that U , N_a and α are not uniquely determined since they depend on the block-encoding technique. Then, various methods have been proposed [5, 30]. One of them is the linear combination of unitaries (LCU) method [30]. This method is applicable for the Hamiltonian, which is given by $H' = \sum_{j=1}^{N_U} \alpha_j U_j$, where U_j is a unitary operator, N_U is the number of unitary operators, and α_j is a positive constant. When each U_j is implemented with C primitive gates, the unitary U encoding the Hamiltonian requires $\mathcal{O}(N_U C)$ primitive gates and $\mathcal{O}(\log N_U)$ ancillary qubits. In this case, the constant is given as $\alpha = \sum_j \alpha_j$ [30]. In addition, another block-encoding method for general sparse matrices has also been proposed [5, 30]. In general, the Hermite operator H' can be described by means of the encoding technique. For simplicity, we assume that its gate complexity is given as C_U .

In quantum computations with the unitary U , the simple iterative procedure eq. (3) may not be appropriate to construct the k th TPQ state. One of the reasons is the exponential decay in the amplitude of the TPQ state since $\|H'/\alpha\| < 1$. The other is that the phase shifts of the ancillary qubits for each unitary operation eq. (6) yields unphysical results in the system registers after the multiple iterations. To overcome two problems, we make use of the uniform spectral amplification and quantum eigenvalue transformation (QET) techniques.

First, we use the uniform spectral amplification method to avoid the exponential decay in the amplitude of the TPQ state. According to the Theorem 30 in Ref. [5] (which is a generalization of the Theorem 2 in Ref. [31]), for any $\Lambda \in (\|H'\|, \alpha]$, $\delta \in (0, 1 - \frac{\|H'\|}{\Lambda}]$, and $\epsilon \in (0, 1/2)$, there exists a unitary \tilde{U} such that

$$\langle\langle 0|_a \otimes I_s \rangle\rangle \tilde{U}(|0\rangle_a \otimes I_s) = \frac{\tilde{H}'}{\Lambda}, \quad (7)$$

where \tilde{H}' is the approximate matrix of H' . When the error between the i th eigenvalues \tilde{E}'_i and E'_i for \tilde{H}' and H' is bounded as

$$\frac{|\tilde{E}'_i - E'_i|}{\Lambda} < \epsilon, \quad (8)$$

the gate complexity of \tilde{U} is given as

$$\mathcal{O}\left(\frac{\alpha}{\Lambda} \frac{1}{\delta} \log\left(\frac{\alpha}{\Lambda} \frac{1}{\epsilon}\right) \cdot C_U\right). \quad (9)$$

We also make use of the QET [4, 5, 30] to perform the multiple operations \tilde{H}'^k exactly. Let V be a unitary satisfying

$$\langle\langle 0|_a \otimes I_s \rangle\rangle V(|0\rangle_a \otimes I_s) = \left(\frac{\tilde{H}'}{\Lambda}\right)^k, \quad (10)$$

and this operation requires two additional ancillary qubits, k controlled- \tilde{U} gates, and $O(k \log(N_a))$ primitive gates [31]. In this connection, one can use a unitary \tilde{U} instead of controlled- \tilde{U} gates when k is odd.

If $|0\rangle_a$ is observed in the ancillary N_a qubits, one obtains the (normalized) approximate k th TPQ state $|\tilde{\psi}_k\rangle / \sqrt{\langle \tilde{\psi}_k | \tilde{\psi}_k \rangle}$, where

$$|\tilde{\psi}_k\rangle = \left(\frac{\tilde{H}'}{\Lambda}\right)^k |\psi_0\rangle. \quad (11)$$

The success probability, *i.e.* the probability of observing $|0\rangle_a$, is given as

$$\langle \tilde{\psi}_k | \tilde{\psi}_k \rangle = \sum_n |c_n|^2 \left(\frac{\tilde{E}'_n}{\Lambda}\right)^{2k}, \quad (12)$$

where we have taken the eigenstates $\{|n\rangle\}$ of the Hamiltonian H as the basis of the initial TPQ state $|\psi_0\rangle$. To discuss thermodynamic properties at low temperatures, we roughly evaluate the quantity for sufficiently large k as

$$O\left(|c_{\min}|^2 \left(\frac{L - E_{\min}}{\Lambda}\right)^{2k}\right), \quad (13)$$

where we have assumed $\epsilon \ll (L - E_{\min})/2k\Lambda$ to neglect the effect of the approximation. c_{\min} is the coefficient of the eigenstate for E_{\min} in the initial random state and $|c_{\min}|^2 \sim O(1/D)$. Since the squared norm eq. (12) is tiny in any case, we also need to use amplitude amplification technique [5, 32] to complete the implementation of \tilde{H}'^k . It is known that the success probability can be amplified to a constant although the quantum complexity increases inversely proportional to the square root of its success probability. Thus, the number of amplitude amplification steps requires as

$$O\left(\sqrt{D} \left(\frac{\Lambda}{L - E_{\min}}\right)^k\right), \quad (14)$$

where the gate complexity of each step is the gate complexity of V . Combining with the above techniques hierarchically, we construct a quantum algorithm for microcanonical TPQ method, which is explicitly shown in the following.

IV. QUANTUM ALGORITHM

Our algorithm is efficient to multiply a random state by \tilde{H}'^k and obtain the approximate normalized TPQ state on the quantum computer with constant probability. Specifically, given a precision parameter $\epsilon' \in (0, O(L - E_{\max}))$, one can construct a unitary \tilde{V} that satisfies

$$\frac{\langle \langle 0|_a \otimes I_s \rangle \tilde{V} (|0\rangle_a \otimes |\psi_0\rangle) \rangle}{\| \langle \langle 0|_a \otimes I_s \rangle \tilde{V} (|0\rangle_a \otimes |\psi_0\rangle) \|} = \frac{|\tilde{\psi}_k\rangle}{\sqrt{\langle \tilde{\psi}_k | \tilde{\psi}_k \rangle}} \quad (15)$$

and

$$\left\| \frac{|\tilde{\psi}_k\rangle \langle \tilde{\psi}_k|}{\langle \tilde{\psi}_k | \tilde{\psi}_k \rangle} - \frac{|\psi_k\rangle \langle \psi_k|}{\langle \psi_k | \psi_k \rangle} \right\|_1 < \epsilon', \quad (16)$$

by using the uniform spectral amplification, QET, and amplitude amplification techniques. The condition on the trace distance in eq. (16) means that no measurement can distinguish between $|\tilde{\psi}_k\rangle / \sqrt{\langle \tilde{\psi}_k | \tilde{\psi}_k \rangle}$ and $|\psi_k\rangle / \sqrt{\langle \psi_k | \psi_k \rangle}$ with probability greater than ϵ' [33]. From the relation between ϵ and ϵ' discussed in Appendix A, one can get the TPQ state with the desired precision in eq. (16) if the error ϵ satisfies

$$\epsilon < \frac{\epsilon'}{4k\Lambda} \frac{\sqrt{\langle \psi_0 | H'^{2k} | \psi_0 \rangle}}{\|H'^{k-1}\|}. \quad (17)$$

Therefore, we can conclude our algorithm in terms of the gate complexity as follows.

Theorem *There exists a quantum circuit \tilde{V} to prepare the k th TPQ state approximately, and the gate complexity of the unitary \tilde{V} is then given as*

$$O\left(\left(\frac{\Lambda}{L - E_{\min}}\right)^k \sqrt{D} \cdot k \cdot \frac{\alpha}{\Lambda} \frac{1}{\delta} \log\left(\frac{k\alpha}{\epsilon'} \frac{\|H'^{k-1}\|_1}{\sqrt{\langle \psi_0 | H'^{2k} | \psi_0 \rangle}}\right) \cdot C_U\right). \quad (18)$$

Replacing $\langle \psi_0 | H'^{2k} | \psi_0 \rangle$ by its average, we get

$$\frac{\|H'^{k-1}\|_1}{\sqrt{\langle \psi_0 | H'^{2k} | \psi_0 \rangle}} \sim \frac{\sum_n E_n'^{k-1}}{\sqrt{\frac{1}{D} \sum_n E_n'^{2k}}} < \frac{D}{l - E_{\max}}. \quad (19)$$

Thus, the gate complexity follows as

$$O\left(\left(\frac{\Lambda}{L - E_{\min}}\right)^k \sqrt{D} \cdot k \cdot \frac{\alpha}{\Lambda} \frac{1}{\delta} \log\left(\frac{k\alpha}{\epsilon'} \frac{D}{l - E_{\max}}\right) \cdot C_U\right). \quad (20)$$

In addition, if the ground state energy has already been obtained precisely, we can set $\Lambda = L - E_{\min}(1 \pm \delta')$ where $\delta' > 0$ is a precision parameter, and the sign is taken so that $\Lambda > L - E_{\min}$. When δ' is chosen to be small [$\delta' \ll 1/k$], the exponential increase with respect to k can be neglected and the gate complexity is then given as

$$O\left(\sqrt{D} k \frac{\alpha}{\Lambda} \frac{1}{\delta} \log\left(\frac{k\alpha}{\epsilon'} \frac{D}{L - E_{\max}}\right) C_U\right). \quad (21)$$

This means that the precision of the ground energy of the Hamiltonian plays a crucial role and the exponential increase of the complexity can be suppressed in the case with $\delta' = O(1/k)$.

More specifically, in the case of the $S = 1/2$ quantum spin systems, where the Hamiltonian is, in general, represented by linear combination of tensor products of Pauli operators, we have $\alpha = O(N)$, $N_U = O(N)$, and $C = O(1)$ by means of the LCU method. Note that $\delta = O(1/k)$, $\Lambda = O(N)$ and $k = O(N)$, the gate complexity is given as

$$O\left(\sqrt{D} \text{polylog}(D) \log\left(\frac{1}{\epsilon'(L - E_{\max})}\right)\right). \quad (22)$$

Since the computational complexity for one iteration of the TPQ method on the classical computer which is constructed by vector and (sparse) matrix operation is $O(D)$, a quadratic

speedup should be realized more or less except for the polylog factors. As for the memory, the TPQ state is stored in N qubits, which is much smaller than the complex vector with D elements in the classical computation. Therefore, our scheme has a potential method to evaluate statistical-mechanical quantities in large systems.

Our quantum algorithm to obtain the k th TPQ state is explicitly shown as follows. We first set constants $L(> E_{\max})$ and $\Lambda(\sim L - E_{\min})$. We also set the accuracy parameter $\epsilon = O(L - E_{\max})$. The TPQ method on quantum computers is composed of three basic steps. The first step is the preparation of the initial random state $|\psi_0\rangle$, which can be obtained from the application of a random circuit [34–37]. The second step is to apply the unitary \hat{V} to the initial state. The last step is to measure the ancillary register to obtain the k th TPQ state. When the state $|0\rangle_a$ is observed in the ancillary qubits, one obtains the TPQ state $|\tilde{\psi}_k\rangle$ in the system register.

Now, we calculate the squared norm $\langle\psi_k|\psi_k\rangle/\Lambda^{2k}$, which is directly related to the complexity of our scheme, to demonstrate the quantity is $O(1/D)$ if δ' is chosen to be $O(1/k)$. To this end, we consider the Heisenberg model on the Kagome lattice (KH model) and Kitaev models with a coupling constant J , as examples of the frustrated quantum spin systems. In these cases, the corresponding Hamiltonians can be easily encoded by the LCU method with $\alpha = L + 3JN/2$ and $\alpha = L + 6JN$, respectively. The details of these models will be explained in Appendix B. Here, the TPQ simulations are performed from 25 independent samples of $|\psi_0\rangle$ on the classical computer, by setting the parameter $L = E_{\max} + \eta$ with $\eta = 0.001N$. Figure 1 shows the squared norm $\langle\psi_k|\psi_k\rangle/\Lambda^{2k}$ for both models with $N = 30$. When the bare TPQ method is applied without the uniform spectral amplification technique, the squared norm rapidly decreases since $L - E_{\min} < \alpha$. This is clearly shown as the dotted line in Fig. 1. On the other hand, we find that the squared norm decreases slowly with small δ' , and is $O(1/D)$ in a region $k \in [0, O(1/\delta')]$ for any δ' . This suggests that preknowledge of E_{\min} with a precision of $O(1/k)$ suppresses the exponential decay in the success probability. The inset of Fig. 1 shows the temperature as a function of k in the TPQ simulations. It is found that the increase of k monotonically decreases the temperature. In general, there exists the characteristic temperature T^* which depends on the model. Namely, $T^* \sim 0.2J$ for the KH model and $T^* \sim 0.03J$ for the Kitaev model (see Appendix B). It is found that $k \sim 1500$ ($50N$) iterations are enough to reach the characteristic temperature. These results imply that the thermodynamic properties can be discussed within a reasonable computational cost. It is expected that our quantum scheme is applied to frustrated quantum spin systems and their interesting low-temperature properties are clarified.

V. SUMMARY

We have presented the quantum algorithm for the TPQ method [11], combining with the block-encoding, uniform spectral amplification, QET, and amplitude amplification techniques. When the precise value of the ground state energy

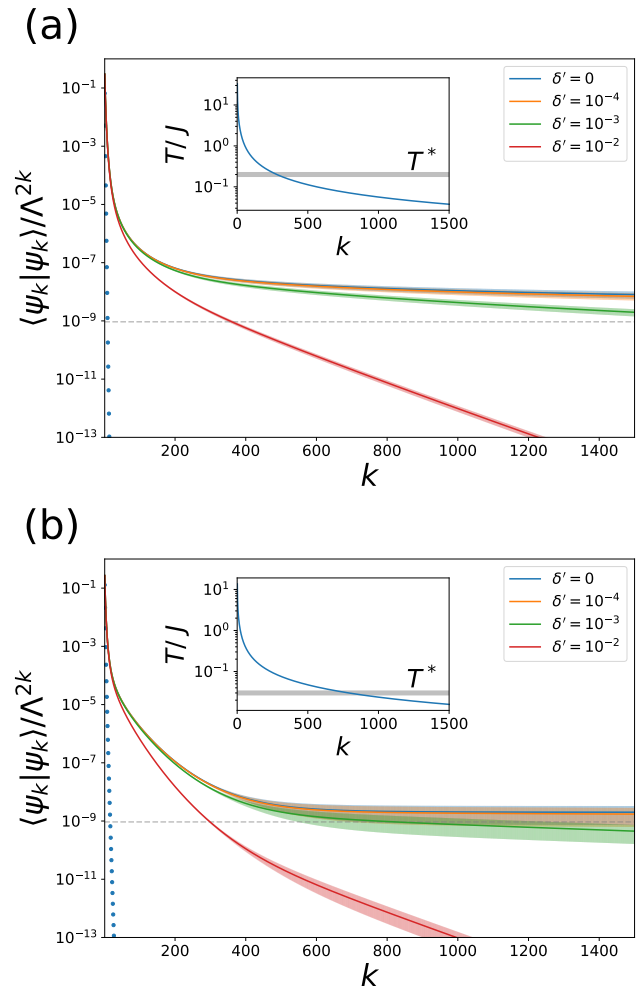


FIG. 1. The squared norm $\langle\psi_k|\psi_k\rangle/\Lambda^{2k}$ as a function of k in (a) the KH and (b) Kitaev models with $N = 30$ when $\delta' = 0, 10^{-4}, 10^{-3}$, and 10^{-2} . The shaded areas stand for the standard deviation of the results. The TPQ results without the uniform spectral amplification is represented by dotted line. The gray dashed line represents $1/D = 2^{-30}$.

is given as an input parameter, the complexity in the multiple products of the Hamiltonian constructing the TPQ states is exponentially reduced. This enables us a quadratic speedup except for the polylog factors compared with the classical simulation. Furthermore, our quantum scheme has an advantage in storing the TPQ state in the computational memory. Therefore, our work should stimulate the further theoretical studies in the condensed matter physics with quantum computer.

ACKNOWLEDGMENTS

We would like to thank K. Fujii for valuable discussions. This work was supported by Grant-in-Aid for Scientific Research from JSPS, KAKENHI Grant Nos. JP22K03525, JP21H01025, JP19H05821 (A.K.).

Appendix A: Relation between ϵ and ϵ'

In this section, we consider the relationship between the approximation error ϵ' given in eq. (8) and the error ϵ between H' and \tilde{H}' in eq. (16), and evaluate the necessary condition for ϵ to achieve the desired precision ϵ' .

First, for any state $|\psi\rangle$ which satisfies $\langle\psi|\psi\rangle = 1$, we define W_k as

$$W_k = \frac{\tilde{H}'^k |\psi\rangle \langle\psi| \tilde{H}'^k}{\tilde{N}_k} - \frac{H'^k |\psi\rangle \langle\psi| H'^k}{N_k}, \quad (\text{A1})$$

where $\tilde{N}_k = \langle\psi|\tilde{H}'^{2k}|\psi\rangle$, and $N_k = \langle\psi|H'^{2k}|\psi\rangle$. Then, we obtain

$$\frac{1}{2} \|W_k\|_1 \quad (\text{A2})$$

$$\leq \frac{1}{2} \left\{ \left\| \frac{1}{\tilde{N}_k} (\tilde{H}'^k - H'^k) |\psi\rangle \langle\psi| \tilde{H}'^k \right\|_1 + \left\| \frac{1}{N_k} H'^k |\psi\rangle \langle\psi| (H'^k - \tilde{H}'^k) \right\|_1 \right\} \quad (\text{A3})$$

$$= \frac{1}{2} \left(\frac{1}{\sqrt{\tilde{N}_k}} + \frac{1}{\sqrt{N_k}} \right) \sum_n |\tilde{E}'_n{}^k - E'_n{}^k|. \quad (\text{A4})$$

From $|\tilde{E}'_n - E'_n|/\Lambda < \epsilon$, assuming that $\epsilon \leq \frac{4}{9} \frac{l-E_{\max}}{k\Lambda}$, the following inequations hold,

$$\sum_n |\tilde{E}'_n{}^k - E'_n{}^k| \leq 2k\Lambda \epsilon \|H'^{k-1}\|_1, \quad (\text{A5})$$

$$\frac{1}{\sqrt{\tilde{N}_k}} \leq \frac{3}{\sqrt{N_k}}. \quad (\text{A6})$$

Thus, we can obtain the upper bound of the above quantity as

$$\frac{1}{2} \|W_k\|_1 \leq 4k\Lambda \epsilon \frac{\|H'^{k-1}\|_1}{\sqrt{N_k}} \quad (\text{A7})$$

Therefore, when $\frac{1}{2} \|W_k\|_1 < \epsilon'$, the error ϵ between the eigenvalues in H' and \tilde{H}' should satisfy

$$\epsilon < \frac{\epsilon'}{4k\Lambda} \frac{\sqrt{N_k}}{\|H'^{k-1}\|_1}. \quad (\text{A8})$$

Here, note that since $\epsilon \leq \frac{4}{9} \frac{l-E_{\max}}{k\Lambda}$ must be satisfied, we should choose ϵ' satisfying $\epsilon' \in (0, \mathcal{O}(L - E_{\max})]$.

Appendix B: Details of the frustrated quantum spin models

Here, we explain the details of the models used in the TPQ simulations. In the frustrated spin systems, low energy states should play an important role and the characteristic temperatures is relatively low, compared to unfrustrated systems. In fact, low-temperature peak or shoulder in the specific heat has been discussed in some systems. Now, we treat the KH and Kitaev model as examples of the frustrated models. To make our discussions clear, we set $L = E_{\max} + \eta$ with $\eta = 0.001N$

1. The Heisenberg model on the Kagome lattice

First, we consider the KH model with antiferromagnetic couplings as one of the systems with geometrical frustration, which is schematically shown in Fig. 2. The system includes triangle structures and each site connects four nearest neighbor sites. The model Hamiltonian is given as

$$H = J \sum_{\langle ij \rangle} \sigma_i \cdot \sigma_j, \quad (\text{B1})$$

where $\sigma_i = (\sigma_i^x, \sigma_i^y, \sigma_i^z)$, σ_i^μ is the μ component of the Pauli matrix at the i th site and the index $\langle ij \rangle$ represents the summation over the connecting spin pairs. $J (> 0)$ is the antiferromagnetic exchange coupling.

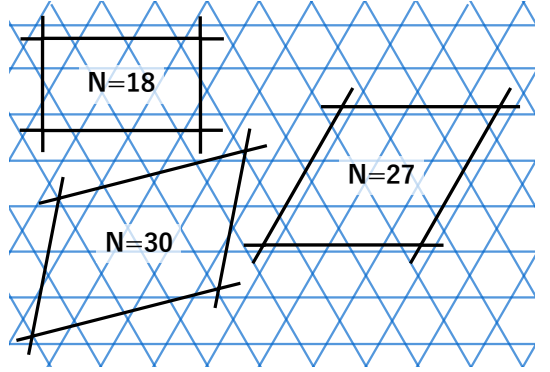


FIG. 2. Finite size clusters of the Kagome lattice used in the TPQ simulations. The boundaries exhibit the periodic boundary conditions.

For the clusters with $N = 18$ and 27 , we evaluate temperatures and internal energies by means of 100 independent TPQ states. By contrast, the numerical cost is high for the cluster with $N = 30$, and 25 independent states are treated. The internal energy is shown in Fig. 3. At low temperatures, the internal energy strongly depends on the size and/or shape of the system. This means that low energy states play an important role in the Kagome-Heisenberg model. It has been clarified that there exists shoulder behavior in the specific heat and its characteristic temperature is deduced as $T^* \sim 0.3J$ [12]. The inset of Fig. 3 shows the temperature as a function of the scaled iteration k/N . We find that the curves little depend on k/N . Therefore, the TPQ state at $T = T^*$ is obtained with $k \sim 10N$ when the parameters are appropriately given.

2. The Kitaev model on the honeycomb lattice

We consider the Kitaev model on the honeycomb lattice [38], which is composed of the direction dependent Ising-like interactions and is known as the exactly solvable systems with bond frustration. The Hamiltonian is given by

$$H = -J \sum_{\langle i,j \rangle_x} \sigma_i^x \sigma_j^x - J \sum_{\langle i,j \rangle_y} \sigma_i^y \sigma_j^y - J \sum_{\langle i,j \rangle_z} \sigma_i^z \sigma_j^z, \quad (\text{B2})$$

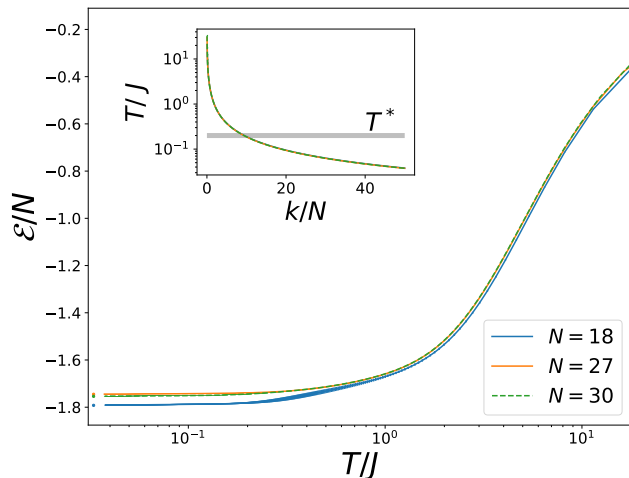


FIG. 3. Internal energy in the Heisenberg model on the Kagome lattice with $N = 18, 27$, and 30 . The inset shows the temperature as a function of k . The error bars stand for the standard deviation of the results. Circles represent the ground state energies for the corresponding system.

where $\langle i, j \rangle_\mu$ represents the nearest-neighbor pair on the $\mu (= x, y, z)$ -bonds. The x -, y -, and z -bonds are shown as red, blue, and green lines in Fig. 4(a). J is the exchange coupling be-

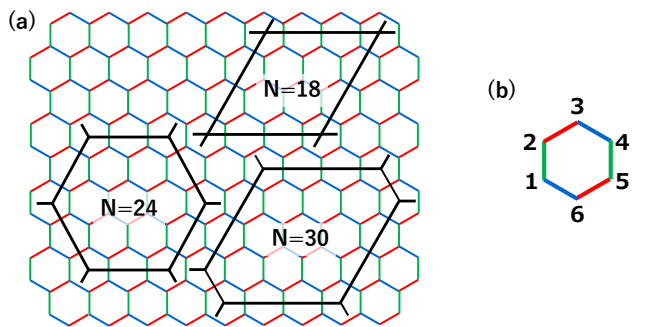


FIG. 4. (a) Finite size clusters of the Kitaev model on the honeycomb lattice used in the TPQ simulations. The boundaries exhibit the periodic boundary conditions. Red, blue, and green lines represent x -, y -, and z -bonds, respectively. (b) Plaquette with sites marked 1–6 is shown for the corresponding operator W_p (see text).

tween the nearest-neighbor spins. In the Kitaev model, there exists a local conserved quantity defined at each plaquette p composed of the sites labeled as $1, 2, \dots, 6$ [see Fig. 4(b)] $W_p = \sigma_1^x \sigma_2^y \sigma_3^z \sigma_4^x \sigma_5^y \sigma_6^z$. It is known that due to the existence of the local conserved quantities, the ground state is the quantum spin liquid, where the spin degrees of freedom is fractionalized into itinerant Majorana fermions and fluxes. This leads to two distinct characteristic energy scales. In fact, we find in Fig. 5 two shoulder structures appear in the internal energy around $T \sim 0.1J$ and $\sim 0.8J$. This behavior is clearly found as a double-peak structure in the specific heat [9], and these peaks are located at $T^*/J \sim 0.03$ and $T^{**}/J \sim 1.5$. The

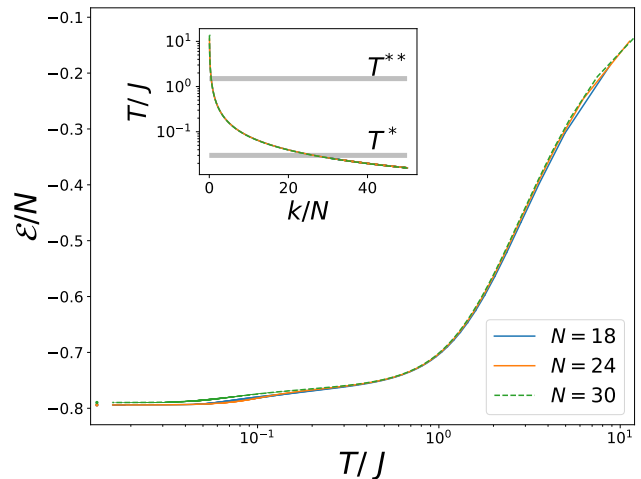


FIG. 5. Internal energy in the Kitaev model with $N = 18, 24$ and 30 . The inset shows the temperature as a function of k . The results are obtained from the TPQ state generated from 100 and 25 samples of the initial random state for $N = 18, 27$, and $N = 30$, respectively, and the error bars stand for the standard deviation of the results. Circles represent the ground state energies for the corresponding system.

characteristic temperature T^* is relatively low due to this fractionalization phenomenon. The inset of Fig. 5 shows that the temperature as a function of k/N . We find that the curve of the temperatures is well scaled by k/N , which is similar to that for the KH model. Therefore, the TPQ state at the lower characteristic temperature $T = T^*$ is obtained with $k \sim 30N$ when appropriate parameters are given.

[1] P. W. Shor, *SIAM Journal on Computing* **26**, 1484 (1997).
 [2] A. W. Harrow, A. Hassidim, and S. Lloyd, *Phys. Rev. Lett.* **103**, 150502 (2009).
 [3] A. M. Childs, R. Kothari, and R. D. Somma, *SIAM Journal on Computing* **46**, 1920 (2017).
 [4] J. M. Martyn, Z. M. Rossi, A. K. Tan, and I. L. Chuang, *PRX Quantum* **2**, 040203 (2021).
 [5] A. Gilyén, Y. Su, G. H. Low, and N. Wiebe, in *Proceedings of the 51st Annual ACM SIGACT Symposium on Theory of Computing* (2019) pp. 193–204.

[6] F. Arute, K. Arya, R. Babbush, D. Bacon, J. C. Bardin, R. Barends, R. Biswas, S. Boixo, F. G. S. L. Brandao, D. A. Buell, B. Burkett, Y. Chen, Z. Chen, B. Chiaro, R. Collins, W. Courtney, A. Dunsworth, E. Farhi, B. Foxen, A. Fowler, C. Gidney, M. Giustina, R. Graff, K. Guerin, S. Habegger, M. P. Harrigan, M. J. Hartmann, A. Ho, M. Hoffmann, T. Huang, T. S. Humble, S. V. Isakov, E. Jeffrey, Z. Jiang, D. Kafri, K. Kechedzhi, J. Kelly, P. V. Klimov, S. Knysh, A. Korotkov, F. Kostritsa, D. Landhuis, M. Lindmark, E. Lucero, D. Lyakh, S. Mandrà, J. R. McClean, M. McEwen, A. Megrant, X. Mi,

- K. Michielsen, M. Mohseni, J. Mutus, O. Naaman, M. Neeley, C. Neill, M. Y. Niu, E. Ostby, A. Petukhov, J. C. Platt, C. Quintana, E. G. Rieffel, P. Roushan, N. C. Rubin, D. Sank, K. J. Satzinger, V. Smelyanskiy, K. J. Sung, M. D. Trevithick, A. Vainsencher, B. Villalonga, T. White, Z. J. Yao, P. Yeh, A. Zalcman, H. Neven, and J. M. Martinis, *Nature* **574**, 505 (2019).
- [7] P. Ball, *Nature* **599**, 542 (2021).
- [8] T. Nakamura, *Phys. Rev. B* **57**, R3197 (1998).
- [9] J. Nasu, M. Udagawa, and Y. Motome, *Phys. Rev. B* **92**, 115122 (2015).
- [10] A. N. Chowdhury and R. D. Somma, *Quantum Inf. Comput.* **17**, 41 (2017).
- [11] S. Sugiura and A. Shimizu, *Phys. Rev. Lett.* **108**, 240401 (2012).
- [12] S. Sugiura and A. Shimizu, *Phys. Rev. Lett.* **111**, 010401 (2013).
- [13] C. Powers, L. B. Otfelie, and D. W. A. Camps, de Jong, arXiv preprint arXiv:2109.01619 (2022).
- [14] L. Coopmans, Y. Kikuchi, and M. Benedetti, arXiv preprint arXiv:2206.05302 (2022).
- [15] Z. Davoudi, N. Mueller, and C. Powers, (2022), 10.48550/ARXIV.2208.13112.
- [16] K. Seki and S. Yunoki, (2022), 10.48550/ARXIV.2207.01782.
- [17] Y. Yamaji, T. Suzuki, T. Yamada, S.-i. Suga, N. Kawashima, and M. Imada, *Phys. Rev. B* **93**, 174425 (2016).
- [18] H. Endo, C. Hotta, and A. Shimizu, *Phys. Rev. Lett.* **121**, 220601 (2018).
- [19] T. Suzuki and Y. Yamaji, *J. Phys. Soc. Jpn.* **88**, 115001 (2019).
- [20] R. Schäfer, I. Hagymási, R. Moessner, and D. J. Luitz, *Phys. Rev. B* **102**, 054408 (2020).
- [21] T. Shimokawa, *Phys. Rev. B* **103**, 134419 (2021).
- [22] H. Tomishige, J. Nasu, and A. Koga, *Phys. Rev. B* **97**, 094403 (2018).
- [23] A. Koga, S. Nakauchi, and J. Nasu, *Phys. Rev. B* **97**, 094427 (2018).
- [24] A. Koga, H. Tomishige, and J. Nasu, *J. Phys. Soc. Jpn.* **87**, 063703 (2018).
- [25] J. Oitmaa, A. Koga, and R. R. P. Singh, *Phys. Rev. B* **98**, 214404 (2018).
- [26] A. Koga and J. Nasu, *Phys. Rev. B* **100**, 100404(R) (2019).
- [27] C. Hickey and S. Trebst, *Nat. Comm.* **10**, 530 (2019).
- [28] K. Morita and T. Tohyama, *Phys. Rev. Research* **2**, 013205 (2020).
- [29] H. Taguchi, Y. Murakami, and A. Koga, *Phys. Rev. B* **105**, 125137 (2022).
- [30] G. H. Low and I. L. Chuang, *Quantum* **3**, 163 (2019).
- [31] G. H. Low and I. L. Chuang, arXiv preprint arXiv:1707.05391 (2017).
- [32] L. K. Grover, in *Proceedings of the twenty-eighth annual ACM symposium on Theory of computing* (1996) pp. 212–219.
- [33] C. W. Helstrom, *Journal of Statistical Physics* **1**, 231 (1969).
- [34] F. Arute, K. Arya, R. Babbush, D. Bacon, J. C. Bardin, R. Barends, R. Biswas, S. Boixo, F. G. Brandao, D. A. Buell, *et al.*, *Nature* **574**, 505 (2019).
- [35] J. Richter and A. Pal, *Physical Review Letters* **126**, 230501 (2021).
- [36] S. Boixo, S. V. Isakov, V. N. Smelyanskiy, R. Babbush, N. Ding, Z. Jiang, M. J. Bremner, J. M. Martinis, and H. Neven, *Nature Physics* **14**, 595 (2018).
- [37] J. Emerson, Y. S. Weinstein, M. Saraceno, S. Lloyd, and D. G. Cory, *science* **302**, 2098 (2003).
- [38] A. Kitaev, *Ann. Phys.* **321**, 2 (2006).